A Quantum Mechanical Study on the Electrostratic Interactions of Poly(L-lysine)·Alkyl Sulfate Complexes

Carlos Alemán,*,† David Zanuy,‡ and Jordi Casanovas§

Departament d'Enginyeria Química, E.T.S. d'Enginyers Industrials de Barcelona, Universitat Politècnica de Catalunya, Diagonal 647, 08028 Barcelona, Spain, Laboratory of Experimental and Computational Biology, National Cancer Institute at Frederick, Building 469, Room 147, Frederick, Maryland 21702, and Departament de Química, Escola Universitària Politècnica, Universitat de Lleida, c/Jaume II n° 69, 25001 Lleida, Spain

Received: November 15, 2002; In Final Form: March 14, 2003

We report a quantum mechanical study on the electrostatic interactions found in poly(L-lysine)·alkyl sulfate complexes, which are materials with interesting technological properties able to adopt self-assembled supramolecular structures. For this purpose, 19 reduced complexes were considered in the gas phase, chloroform solution, and aqueous solution. Calculations in the gas phase were carried out up to the MP2/6-311++G(d,p) level, while the influence of the bulk solvent was investigated at the HF/6-311++G(d,p) level using the polarizable continuum model. The electrostatic interaction characteristics of poly(L-lysine)·alkyl sulfate complexes have been compared with those of alkyltrimethylammonium·poly(α,L-glutamate) complexes, a related family of materials previously investigated.

1. Introduction

The interaction between an ammonium cation and a carboxylate anion with the formation of an ion-pair complex is a common process in protein chemistry. These ion pairs, usually denoted *salt bridges*, are involved in large variety of biological processes.[1] Understanding of the structural and functional roles played by salt bridges cannot be achieved without knowledge of the energetics of this interaction. Accordingly, a number of theoretical studies have been devoted to investigating salt bridges through sophisticated quantum mechanical methods on reduced systems.[2]

For the past decade, the interest in ion-pair interactions has been extended to materials science. Thus, remarkable advances in noncovalent chemistry have led to design of new materials consisting of charged polymer chains (polyelectrolytes) and oppositely charged small amphiphilic molecules.[3−6] Most work in this area has involved polypeptides able to adopt highly ordered secondary structures.[3,4] Within this context, we are interested in complexes formed by synthetic sodium poly(α,L-glutamate) and oppositely charged alkyltrimethylammonium surfactants, abbreviated *n*-ATMA·PALG, where *n* denotes the number of carbon atoms of the alkyl group.

These materials were extensively studied by Tirrell's group in both the solid state and dilute chloroform solution.[3] The more relevant features of the electrostatic interactions involved in *n*-ATMA·PALG complexes were investigated using ab initio quantum mechanical methods on reduced systems constituted by simple organic molecules, that is, acetate anion (CH_3COO^-) and alkyltrimethylammonium cations [$(CH_3)_3-N^+-(CH_2)_{n-1}-CH_3$ with *n* ranging from 1 to 4].[7] Results were employed to develop a suitable force field to model *n*-ATMA·PALG complexes in dilute chloroform solution using atomistic molecular dynamics simulations and explicit solvent molecules.[8]

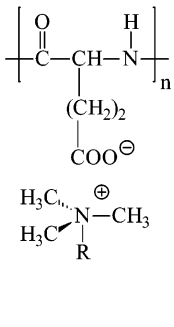

***n*-ATMA·PALG**

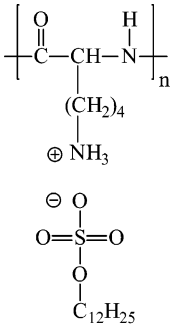

PLL·*n*-AS

We are also interested in the polypeptide−surfactant complexes consisting of poly(L-lysine) and the oppositely charged alkyl sulfate surfactants, abbreviated PLL·*n*-AS. The most remarkable difference between these materials, which were also experimentally investigated by Tirrell's group,[3c,4] and the *n*-ATMA·PALG ones involves the distribution of the charged groups. Thus, in the latter compounds, the polypeptide chain and the surfactant molecules are negatively and positively charged, respectively, while the opposite situation occurs for PLL·*n*-AS complexes. However, to the best of our knowledge, there has so far been no attempt to analyze the implications of such difference in the electrostatic interaction between the polyelectrolyte and the surfactants.

Following our previous theoretical studies on *n*-ATMA·PALG complexes, we present here a systematic quantum mechanical study about the geometry and energetics of the electrostatic interaction found in PLL·*n*-AS complexes. Interaction energies have been computed not only in the gas phase but also in chloroform and aqueous solutions. Results have been compared with those previously reported for the electrostatic interactions of *n*-ATMA·PALG complexes[7] and the salt bridges of proteins.[2]

* To whom correspondence should be addressed. E-mail: carlos.aleman@upc.es.
† Universitat Politècnica de Catalunya.
‡ National Cancer Institute at Frederick.
§ Universitat de Lleida.

10.1021/jp027467b CCC: $25.00
Published on Web 04/26/2003

2. Methods

The structures of both complexes and monomers were determined in the gas phase by full geometry optimizations at the MP2/6-31G(d) level of theory. It should be noted that the 6-31G(d) basis set[9] provides geometries very similar to those obtained with larger basis sets, even in systems constituted by charged monomers.[2b,10] The complexes constituted by the smaller model molecules were verified as true minima on the potential energy hypersurface by the analytical calculation of their force constants.

To present a systematic study, single-point calculations were performed for all the complexes and monomers at the HF/6-311G(d,p), HF/6-311++G(d,p), MP2/6-311G(d,p), MP2/6-311++G(d,p), and MP4/6-31G(d,p) levels of theory. The stabilization energy in the gas phase, $E_{stab,g}$, was calculated according to eq 1.

$$E_{stab,g} = E_{ab} - E_{a,comp} - E_{b,comp} \quad (1)$$

where E_{ab} corresponds to the total energy of the optimized complex while $E_{a,comp}$ and $E_{b,comp}$ are the energies of the isolated monomers with the geometries obtained from the optimization of the complex. The counterpoise (CP) method was applied to correct the basis set superposition error (BSSE).[11] The CP correction for each monomer was calculated as the difference between the energy of the monomer on the complexed geometry with the basis set of the whole complex and that of the same monomer without ghost orbitals.

The distortion energy, E_{dis}, which estimates the relaxation of the monomers on ion-pair formation, was computed by using eq 2.

$$E_{dis} = (E_{a,comp} + E_{b,comp}) - (E_{a,opt} + E_{b,opt}) \quad (2)$$

where $E_{a,opt}$ and $E_{b,opt}$ are the energies obtained from the geometries optimized for the isolated monomers. Thus, the total interaction energies in the gas phase, $E_{int,g}$, were evaluated as the sum of the stabilization and distortion energies.

$$E_{int,g} = E_{stab,g} + E_{dis} \quad (3)$$

The influence of the corrections for zero-point energy and entropy on $E_{int,g}$ was investigated for the smaller complexes using frequencies calculated at the MP2/6-31G(d) level.

The effect of the solvent (water and chloroform) on the interaction energies was estimated following the polarizable continuum model (PCM) developed by Miertus, Scrocco, and Tomasi.[12] PCM calculations were performed in the framework of the ab initio HF level with the 6-311++G(d,p) basis set and using the gas-phase optimized geometries. The interaction energy in aqueous and chloroform solution, $E_{int,aq/chl}$, was evaluated by using eq 4.

$$E_{int,aq/chl} = E_{int,g} + \Delta\Delta G_{assoc} \quad (4)$$

where $\Delta\Delta G_{assoc}$ is the difference between the free energy of solvation of the ion pair, $\Delta G_{sol,ab}$, and those of the separated monomers, $\Delta G_{sol,a}$ and $\Delta G_{sol,b}$, in the corresponding solvent.

$$\Delta\Delta G_{assoc} = \Delta G_{sol,ab} - \Delta G_{sol,a} - \Delta G_{sol,b} \quad (5)$$

All of the calculations were performed with Gaussian 98, revision A.7,[13] on an IBM/SP2 at the Centre de Supercomputació de Catalunya (CESCA).

TABLE 1: Chemical Constitution of the Ion-Pair and Neutral Complexes Investigated in This Work

complex	cation	anion
I	$CH_3-NH_3^+$	$CH_3-O-SO_3^-$
II	$CH_3-CH_2-NH_3^+$	$CH_3-O-SO_3^-$
III	$CH_3-(CH_2)_2-NH_3^+$	$CH_3-O-SO_3^-$
IV	$CH_3-(CH_2)_3-NH_3^+$	$CH_3-O-SO_3^-$
V	$HCO-CH-(CH_2)_4-NH_3^+-NH_2$	$CH_3-O-SO_3^-$
VI	$CH_3-CH_2-NH_3^+$	$CH_3-CH_2-O-SO_3^-$
VII	$CH_3-(CH_2)_2-NH_3^+$	$CH_3-CH_2-O-SO_3^-$
VIII	$CH_3-CH_2-NH_3^+$	$CH_3-(CH_2)_2-O-SO_3^-$
IX	$CH_3-(CH_2)_2-NH_3^+$	$CH_3-(CH_2)_2-O-SO_3^-$
X	$CH_3-CH_2-NH_3^+$	$CH_3-(CH_2)_3-O-SO_3^-$
XI	$CH_3-(CH_2)_2-NH_3^+$	$CH_3-(CH_2)_3-O-SO_3^-$
XII	$CH_3-CH_2-NH_3^+$	$CH_3-(CH_2)_4-O-SO_3^-$
XIII	$CH_3-(CH_2)_2-NH_3^+$	$CH_3-(CH_2)_4-O-SO_3^-$
XIV	$CH_3-CH_2-NH_3^+$	$CH_3-(CH_2)_5-O-SO_3^-$
XV	$CH_3-(CH_2)_2-NH_3^+$	$CH_3-(CH_2)_5-O-SO_3^-$
XVI	Na^+	$CH_3-O-SO_3^-$
XVII	Li^+	$CH_3-O-SO_3^-$
XVIII	$CH_3-NH_3^+$	Cl^-
XIX	$CH_3-NH_3^+$	F^-

3. Results and Discussion

A total of 19 ion pairs have been investigated in this work, which are listed in Table 1 and will be discussed in successive sections. They can be classified in two groups according to their chemical constitution: (i) complexes formed by two molecular ions (from **I** to **XV** in Table 1) and (ii) complexes formed by a molecular ion and an oppositely charged atomic ion (from **XVI** to **XIX** in Table 1). It should be noted that complex **V** provides the best description for the PLL cation, while the *n*-AS surfactants are accurately mimicked in complexes **XIV** and **XV**.

This section is outlined as follows. We first discuss the general effect of the quantum mechanical method, the basis set, and the BSSE on $E_{stab,g}$ and $E_{int,g}$. Second, the strength of the electrostatic interaction involved in PLL·*n*-AS complexes is analyzed in the gas phase. In this context, the influence of describing accurately the PLL and *n*-AS fragments is examined in detail. Furthermore, the results are systematically compared with those obtained for the *n*-ATMA·PALG complexes[7] and proteins.[2] Third, we briefly discuss the geometry of the electrostatic interaction of PLL·*n*-AS complexes. Next, we examine how the binding changes when one of the molecular ions (alkylammonium cation or alkyl sulfate anion) is replaced by a similarly charged atomic ion. After this, we show the influence of the bulk solvent (chloroform and water) on the interaction energy.

3.1. Influence of the Quantum Mechanical Method, the Basis Set, and the BSSE on the Stabilization and Interaction Energies. For the discussion of this section, we will consider the results obtained for all of the molecular ion pairs (**I**−**XVI**), but only two complexes constituted by a molecular ion and an oppositely charged atom (**XVI** and **XVII**). Thus, results for complexes **XVIII** and **XIX** have not been taken into account because, as will be indicated in section 3.4, they are not true minima. Tables 2 and 3 list the values of $E_{stab,g}$ (eq 1) with and without correcting the BSSE, respectively. Finally, Table 4 presents the values of $E_{int,g}$ (eq 3), which take into consideration the geometrical relaxation of the monomers.

The results in Tables 2 and 4 show that, for complexes constituted by two molecular ions, the values of $E_{stab,g}$ and $E_{int,g}$ calculated using the HF theory are slightly underestimated (∼4%) with respect to those obtained at the MP2 level. The opposite effect is detected for complexes **XVI** and **XVII**, for

TABLE 2: Stabilization Energies Computed in the Gas Phase ($E_{stab,g}$, kcal/mol) with Correction for the Basis Set Superposition Error

	MP2			MP4	HF	
complex	6-31G(d)	6-311G(d,p)	6-311++G(d,p)	6-31G(d)	6-311G(d,p)	6-311++G(d,p)
I	−118.5	−117.0	−115.3	−117.9	−111.9	−110.7
II	−116.2	−114.9	−113.3	−115.5	−109.9	−108.9
III	−115.0	−113.7	−112.1	−114.4	−108.7	−107.6
IV	−114.5	−113.2	−111.7		−108.1	−107.0
V	−115.0	−113.8	−112.7		−109.2	−108.4
VI	−116.2	−114.8	−113.5		−110.0	−109.1
VII	−115.1	−113.7	−112.4		−108.8	−107.8
VIII	−116.1	−114.7	−113.4		−109.9	−109.1
IX	−115.0	−112.9	−112.3		−108.7	−107.8
X	−116.1	−114.6	−113.4		−109.9	−109.0
XI	−115.0	−113.5	−112.2		−108.7	−107.8
XII	−116.1	−114.6	−113.3		109.9	−109.0
XIII	−114.9	−113.5	−112.2		−108.7	−107.8
XIV	−116.1	−114.6	−113.3		−109.9	−109.0
XV	−114.9	−113.4	−112.2		−108.6	−107.7
XVI	−135.8	−128.1	−125.2	−131.6	−130.7	−129.1
XVII	−159.1	−155.7	−152.3	−158.8	−157.4	−155.8
XVIII	−116.4	−115.8	−115.5	−116.0	−109.9	−110.2
XIX	−155.0	−154.1	−142.5	−154.2	−150.2	−142.0

TABLE 3: Stabilization Energies Computed in the Gas Phase ($E_{stab,g}$, kcal/mol) without Correction for the Basis Set Superposition Error

	MP2			MP4	HF	
complex	6-31G(d)	6-311G(d,p)	6-311++G(d,p)	6-31G(d)	6-311G(d,p)	6-311++G(d,p)
I	−124.0	−123.7	−120.1	−127.6	−114.8	−112.5
II	−122.6	−122.2	−118.6	−122.3	−113.2	−110.9
III	−121.5	−121.2	−117.7	−121.3	−112.0	−109.7
IV	−120.0	−120.8	−117.4		−111.5	−109.2
V	−120.6	−121.5	−118.8		−112.6	−110.7
VI	−122.6	−122.1	−118.8		−113.3	−111.2
VII	−121.6	−121.1	−118.0		−112.1	−110.0
VIII	−122.5	−121.9	−118.8		−113.2	−111.1
IX	−121.5	−121.0	−117.9		−112.0	−110.0
X	−122.5	−121.9	−118.7		−113.1	−111.1
XI	−121.5	−120.9	−117.8		−112.0	−109.9
XII	−122.5	−121.8	−118.7		−113.1	−111.0
XIII	−121.5	−120.8	−117.8		−111.9	−109.9
XIV	−122.4	−121.8	−118.7		−113.1	−111.0
XV	−121.4	−120.8	−117.8		−111.9	−109.9
XVI	−140.1	−135.1	−128.6	−140.4	−133.5	−130.2
XVII	−168.3	−165.3	−157.5	−168.7	−161.3	−157.5
XVIII	−120.8	−119.3	−120.1	−120.2	−110.5	−110.6
XIX	−176.8	−174.6	−147.7	−176.4	−161.6	−143.0

TABLE 4: Interaction Energies[a] Computed in the Gas Phase ($E_{int,g}$, kcal/mol)

	MP2			MP4	HF	
complex	6-31G(d)	6-311G(d,p)	6-311++G(d,p)	6-31G(d)	6-311G(d,p)	6-311++G(d,p)
I	−113.0	−111.4	−110.0	−112.4	−106.4	−105.4
II	−110.5	−109.2	−107.9	−109.9	−104.8	−104.0
III	−109.4	−108.1	−106.8	−109.4	−103.7	−102.8
IV	−110.0	−107.6	−106.4		−103.1	−102.2
V	−110.0	−107.6	−107.9		−104.1	−103.6
VI	−110.3	−108.8	−107.9		−104.8	−104.1
VII	−109.3	−107.8	−106.9		−103.7	−102.9
VIII	−110.1	−108.6	−107.8		−104.7	−104.1
IX	−109.1	−106.9	−106.8		−103.6	−102.9
X	−110.1	−108.5	−107.7		−104.7	−104.0
XI	−109.1	−107.5	−106.6		−103.6	−102.9
XII	−110.1	−108.5	−107.6		−104.7	−104.0
XIII	−109.0	−107.5	−106.5		−103.6	−102.8
XIV	−110.1	−108.5	−107.7		−104.7	−104.1
XV	−109.0	−107.4	−106.6		−103.5	−102.8
XVI	−131.6	−123.6	−121.2	−127.6	−127.4	−126.0
XVII	−151.3	−147.7	−145.1	−151.3	−150.8	−149.6
XVIII	−115.4	−114.8	−114.5	−115.0	−108.3	−108.6
XIX	−151.4	−150.6	−139.0	−150.5	−145.9	−137.7

[a] $E_{int,g}$ was computed as the sum of the stabilization energies displayed in Table 2 and the distortion energies (see Supporting Information).

which the HF method predicts stronger electrostatic interactions than the MP2 one (∼2−3%). On the other hand, the results derived from Møller−Plesset calculations with single, double, triple, and quadruple excitations (MP4), which were performed only with the 6-31G(d) basis set, were almost identical to those produced at the MP2 level with the same basis set, the largest

difference between the two methods being 0.7 kcal/mol (0.6%). Complex **XVI** was an exception to this behavior; in this case, the values of $E_{stab,g}$ and $E_{int,g}$ computed at the MP4 level were 4.2 (3.1%) and 4.0 kcal/mol (3.0%), respectively, larger than those derived from MP2 calculations.

Inspection of the results obtained with the 6-31G(d), 6-311G-(d,p), and 6-311++G(d,p) basis sets indicates that, for the molecular ion pairs, both $E_{stab,g}$ and $E_{int,g}$ decrease when the size of the basis sets increases. Such energy parameters diminish about 1.5 and 0.5 kcal/mol, respectively, when the basis set is extended from the 6-31G(d) to the 6-311G(d,p). The introduction of diffuse functions to the 6-311G(d,p) basis set produces a new reduction of about 1 kcal/mol. For the complexes containing an atomic ion, the improvement of the basis set produces similar qualitative effects. However, the reduction of $E_{stab,g}$ and $E_{int,g}$ is more pronounced in these complexes than that for the ion pairs formed by two molecules. This feature is especially notorious for complex **XVI**, in which the energy parameters decrease by about 10.5 kcal/mol when the 6-31G(d) basis set is extended to the 6-311++G(d,p) one.

Comparison between results displayed in Tables 2 and 3 indicates that, in general, the size of the BSSE is about 3−4 kcal/mol larger at the MP2 level than at the HF one. The strength of the $E_{stab,g}$ predicted by MP2 calculations is overestimated by about 5−8 kcal/mol when the BSSE is not corrected. Thus, this energy parameter decreases by about 5−6% after introducing the BSSE correction. However, it should be noted that for ion pairs containing small atomic ions, such as Li^+ (**XVII**) or F^- (**XIX**), the size of the BSSE increases notably when a basis set without diffuse functions is used.

The discussion of the next sections will be centered on MP2/6-311++G(d,p) calculations, which provide our best estimation of $E_{stab,g}$ and $E_{int,g}$.

3.2. Energetics of the Electrostatic Interaction of PLL·*n*-AS Complexes in the Gas Phase. First, we get insight into the influence of the model molecules used to mimic the electrostatic interactions of PLL·*n*-AS complexes. The description of the molecular cation was investigated by calculating the complexes formed by the methyl sulfate anion and the alkylammonium cation (alkyl = methyl, **I**; alkyl = ethyl, **II**; alkyl = propyl, **III**; and alkyl = butyl, **IV**). Results are compared in Tables 2 and 4 with those achieved for complex **V**, which is constituted by *N*-formylamino lysine (For-Lys-NH_2) and methyl sulfate.

As can be seen, both $E_{stab,g}$ and $E_{int,g}$ vary as follows: **I** > **II** > **III** > **IV** independently of the level of theory and the basis set. Thus, these energy terms drop 3.6 kcal/mol when the alkyl group changes from methyl to butyl. This reduction must be attributed to the electron leasing associated with the alkyl groups in classical organic chemistry. Very similar results were recently reported for complexes constituted by the acetate anion and an alkyltrimethylammonium cation, with alkyl = methyl, ethyl, propyl, and butyl, which were used to model the electrostatic interactions of *n*-ATMA·PALG complexes.[7a] In such cases, the $E_{int,g}$ computed at the MP2/6-31+G(d) level also decreases 3.6 kcal/mol when the size of the alkyl group increases from methyl to butyl.

Comparison among complexes **I**−**V** indicates that the better description of the For-Lys-NH_2 is provided by the ethylammonium and propylammonium cations. Thus, the value of $E_{stab,g}$ predicted for **V** is overestimated and underestimated by **II** and **III**, respectively, by 0.6 kcal/mol. Because these results do not allow establishment of a clear distinction between the ethylammonium and propylammonium cations, we decided to consider both as model molecules of the PLL fragment.

TABLE 5: Interaction Enthalpies[a] ($H_{int,g}$, kcal/mol) and Free Energies[b] ($G_{int,g}$, kcal/mol) Computed in the Gas Phase for Selected Complexes

complex	ΔZPE	$H_{int,g}$	$-T\Delta S$	$G_{int,g}$
I	0.9	−109.1	2.3	−106.8
II	0.9	−107.0	2.1	−104.9
III	0.8	−106.0	1.9	−104.0
IV	0.9	−107.0	2.8	−104.1

[a] $H_{int,g}$ was estimated by adding the zero-point energy correction term (ΔZPE) computed at the MP2/6-31G(d) level to the $E_{int,g}$ obtained at the MP2/6-311++G(d,p) level (see Table 4). [b] $G_{int,g}$ was estimated by adding the entropy correction ($-T\Delta S$, $T = 298.15$ K) computed at the MP2/6-31G(d) level to the $H_{int,g}$ value.

Next, the influence of the size of the surfactant alkyl group was investigated by comparing the results provided by complexes containing one of the selected alkylammonium cations (alkyl = ethyl, **II**, **VI**, **VIII**, **X**, **XII**, and **XIV**; and alkyl = propyl, **III**, **VII**, **IX**, **XI**, **XIII**, and **XV**) and an alkyl sulfate anion (alkyl = methyl, **II** and **III**; alkyl = ethyl, **VI** and **VII**; alkyl = propyl, **VIII** and **IX**; alkyl = butyl, **X** and **XI**; alkyl = pentyl, **XII** and **XIII**; and alkyl = hexyl, **XIV** and **XV**). It is worth noting that the size of the aliphatic group of the anion has an almost negligible effect in both $E_{stab,g}$ and $E_{int,g}$. For instance, the values of $E_{int,g}$ predicted for complexes **III** and **XV** differ by only 0.2 kcal/mol, although they are constituted by methyl sulfate and hexyl sulfate, respectively. On the other hand, results derived for complexes formed by ethylammonium and propylammonium cations are also very similar, the values of $E_{stab,g}$ and $E_{int,g}$ differing by about 1 kcal/mol (1.0%).

The results obtained for complex **V** indicate that $E_{stab,g}$ and $E_{int,g}$ are −112.7 and −107.9 kcal/mol, respectively, for the electrostatic interaction of PLL·*n*-AS complexes. According to the Tables 2 and 4, it can be concluded that the reduced models considered for complexes **II** and **III** satisfactorily reproduce the energetics of such interaction. The $E_{int,g}$ computed at the MP2/6-31+G(d) level for the complexes formed by the acetate anion and the alkyltrimethylammonium cation range from −97.4 (alkyl = methyl) to −95.0 (alkyl = butyl) kcal/mol.[7] Accordingly, the electrostatic interaction of PLL·*n*-AS complexes is about 13 kcal/mol stronger than that of *n*-ATMA·PALG complexes. This fact can be attributed to (i) the larger concentration of positive charge in the alkylammonium cation with respect to the alkyltrimethylammonium one and (ii) the intermolecular geometry of the complexes, which will be discussed in the next section. On the other hand, the electrostatic interaction in PLL·*n*-AS complexes is slightly weaker than that in salt bridges in proteins. Thus, the $E_{int,g}$ predicted at the MP2/6-31+G(d) for the complex constituted by methylguanidinium cation and the acetate anion range from −117.9 to −108.8 kcal/mol, depending on the intermolecular geometry.[2d]

The influence of the zero-point energy and entropy corrections to the energetics of the electrostatic interaction investigated in this work has been investigated using the frequencies computed at the MP2/6-31G(d) level for complexes **I**, **II**, **III**, and **VI**, as well as for the corresponding isolated monomers. Results are displayed in Table 5. As can be seen, differences in zero-point energies are very small (less than 1 kcal/mol), the change introduced in $E_{int,g}$ being almost negligible. The numerical values of the entropy correction for the four investigated complexes range from 1.9 to 2.8 kcal/mol, the variation introduced in the energetics of the binding being lower than 2.6%. These results indicate that the influence of both the zero-point energy and entropy contributions is very small and, therefore, the omission of these terms should not alter the conclusions presented in this work.

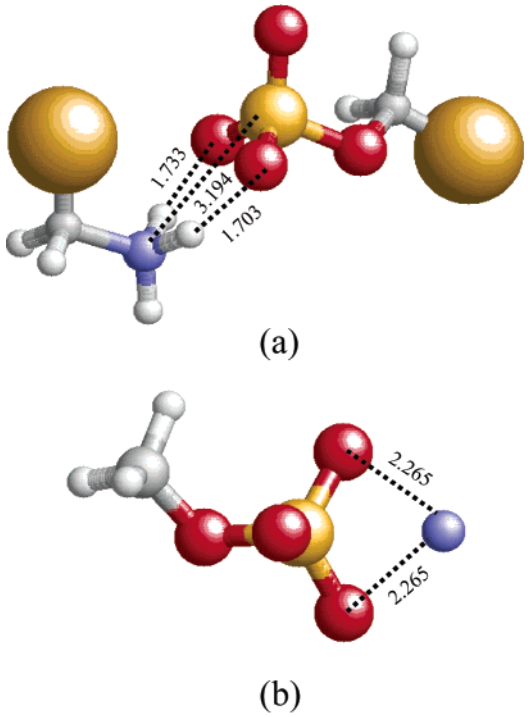

Figure 1. Optimized geometries of the (a) alkylammonium·alkyl sulfate ion pairs (only the atoms involved in the intermolecular interaction have been explicitly represented, the remaining atoms of the alkyl groups being symbolized by large spheres) and (b) complex **XVI**. Intermolecular distances are given in Å.

3.3. Geometry of the Electrostatic Interaction of PLL·*n*-AS Complexes. The optimized intermolecular geometry for this interaction is displayed in Figure 1a. All of the investigated complexes, with exception of **I**, provided almost identical results, as can be inferred from the maximum deviations of the following intermolecular distances and angles: $d(N\cdots S) = 3.194 \pm 0.001$ Å, $d(N-H_1\cdots O_1) = 1.703 \pm 0.004$ Å, $d(N-H_2\cdots O_2) = 1.733 \pm 0.003$ Å, $\angle N\cdots S-O(-C) = 113.2° \pm 0.8°$, and $\angle S\cdots N-C = 116.9° \pm 0.4°$. On the other hand, the small size of the methylammonium cation severely affected the intermolecular parameters obtained for **I**: $d(N\cdots S) = 3.130$ Å, $d(N-H_1\cdots O_1) = 1.709$ Å, $d(N-H_2\cdots O_2) = 1.764$ Å, $\angle N\cdots S-O(-C) = 95.0°$, and $\angle S\cdots N-C = 99.4°$.

Inspection of Figure 1a reveals that the sulfate group is symmetrically arranged with respect to the cation, as can be inferred from the small differences found between the two H···O intermolecular distances (0.030 Å). A completely different situation was found for the model complexes used to investigate *n*-ATMA·PALG complexes, where the two intermolecular distances differ by about 0.12−0.16 Å.[7a] Moreover, atomistic molecular dynamics simulations on realistic models of *n*-ATMA·PALG complexes[8] also evidenced such asymmetric arrangement, which was attributed to a delicate balance between the repulsive and attractive interactions.

Comparison between the intermolecular geometries predicted for PLL·*n*-AS and *n*-ATMA·PALG complexes reveals another interesting feature. The distance between the cation and the anion, which was measured as N(alkylammonium)···S(alkyl sulfate) and N(alkyltrimethylammonium)···C(acetate), respectively, is about 1 Å larger in the latter than in the former complexes.[7] This is in agreement with the relative strength of the corresponding interactions (see section 3.2.).

Finally, it should be mentioned that the aliphatic groups of the alkylammonium cations and the alkyl sulfate anions were initially arranged according to an all-trans conformation. Analysis of the dihedral angles after geometry optimizations indicated that, in all cases, such conformation was preserved.

3.4. Complexes Constituted by a Molecular Ion and an Oppositely Charged Atomic Ion. The $E_{stab,g}$ and $E_{int,g}$ for the complexes constituted by alkyl sulfate and a metal cation, M^+ ($M^+ = Na^+$, **XVI**; $M^+ = Li^+$, **XVII**) are displayed in Tables 2−4. As expected, the interaction is more attractive for complexes involving a metal cation than for those containing an organic molecular cation. Thus, the binding of Na^+ and Li^+ to methyl sulfate is 11.2 and 35.1 kcal/mol (10% and 32%, respectively) stronger than that of methylammonium, respectively. Obviously, these energy differences are due to the greater concentration of the charge in atomic ions than in organic molecular ions.

Figure 1b shows the minimum energy structure obtained for complex **XVI**. The Na^+ is symmetrically arranged with respect to two oxygen atoms of the sulfate moiety, the $Na^+\cdots O$ distance being 2.265 Å. A symmetrical arrangement was also obtained for complex **XVII**, the distances between the metal cation and the oxygen atoms being in this case 0.059 Å shorter than those for **XVI**.

Geometry optimizations were also performed on the ion pairs formed by methylammonium cation and a simple atomic anion, X^- (X = Cl and F). However, in both cases the ion pair was not a "true" energy minimum on the potential energy surfaces and collapses to the neutral complex formed by methylamine and HX. This is consequence of the great concentration of negative charge, which is larger in X^- than in alkyl sulfate anions. The collapse of the ion pair to the neutral complex in geometry optimizations using the 6-31G(d) basis set has been also observed for complexes constituted by formate anion and trimethylammonium cation,[2c] and acetate anion and methylammonium cation.[2d]

To provide an estimation of the $E_{stab,g}$ and $E_{int,g}$ values for the complexes **XVIII** and **XIX**, partial optimizations were performed by imposing the restraints necessary to keep the ionic nature of the two constituents in the complex. As expected, results indicate that the electrostatic interaction becomes stronger when the size of the atomic anion decreases. Furthermore, the strength of the binding is larger for these complexes than for the bimolecular ones.

3.5. Effect of the Solvent in the Formation of the Ion Pair. Table 6 shows the ΔG_{sol}, $\Delta\Delta G_{assoc}$, and E_{int} in water and chloroform for the 19 ion pairs investigated in this work. In all cases, the solvation of the complexes was worse than that of the isolated ions, which led to positive $\Delta\Delta G_{assoc}$ values. Furthermore, the magnitude of such repulsive energy term increases with the polarity of the solvent. Thus, the solvation of the isolated ions in water is favored by strong electrostatic interactions between the bulk solvent and the charged solutes, while in chloroform, the strength of such interactions decreases.

The $E_{int,aq}$ and $E_{int,chl}$ values were obtained by adding the $E_{int,g}$ estimated at the MP2/6-311++G(d,p) level (Table 4) to the $\Delta\Delta G_{assoc}$ term computed in water and chloroform, respectively (eq 4). The results indicate that the complexation process is less favorable in chloroform solution than in the gas phase. Thus, a comparison between the $E_{int,chl}$ and $E_{int,g}$ values reveals that the strength of the binding is about 75% weaker in the former environment than in the latter one. However, it should be emphasized that in chloroform solution the unfavorable $\Delta\Delta G_{assoc}$ term is counterbalanced by the gas-phase contribution leading in all cases to negative $E_{int,chl}$ values. According to the results displayed in Table 6, the binding of an alkylammonium cation to an alkyl sulfate anion in chloroform solution to form the

TABLE 6: Free Energy of Solvation and Interaction Energy[a] in Chloroform ($\Delta G_{sol,chl}$ and $E_{int,chl}$, kcal/mol) and Aqueous ($\Delta G_{sol,aq}$ and $E_{int,aq}$, kcal/mol) Solutions and the Difference between the Free Energy of Solvation of the Ion Pair and the Separated Monomers ($\Delta\Delta G_{assoc}$, kcal/mol)

complex	$\Delta G_{sol,chl}$	$\Delta\Delta G_{assoc}$	$E_{int,chl}$	$\Delta G_{sol,aq}$	$\Delta\Delta G_{assoc}$	$E_{int,aq}$
I	−10.1	83.7	−26.3	−20.6	114.9	4.9
II	−10.1	81.5	−26.4	−20.7	112.1	4.2
III	−8.9	81.7	−25.1	−18.9	113.0	6.2
IV	−7.9	82.4	−24.0	−17.2	115.3	8.9
V	−11.6	82.9	−25.0	−28.5	114.2	6.3
VI	−10.1	80.7	−27.2	−21.2	111.1	3.2
VII	−8.9	81.7	−25.2	−19.2	112.2	5.3
VIII	−9.6	81.3	−26.5	−20.3	111.2	3.4
IX	−8.4	81.5	−25.3	−18.3	112.3	5.5
X	−9.5	80.9	−26.8	−20.1	110.7	3.0
XI	−8.4	81.1	−25.5	−18.3	111.7	5.1
XII	−9.5	80.8	−26.8	−19.7	110.9	3.3
XIII	−8.3	81.0	−25.5	−18.0	111.7	5.2
XIV	−9.4	80.7	−27.0	−19.6	110.4	2.7
XV	−8.3	80.8	−25.8	−17.9	111.2	4.6
XVI	−14.0	90.0	−31.2	−26.9	123.2	2.0
XVII	−10.8	132.0	−13.1	−23.2	149.8	4.7
XVIII	−11.6	92.1	−22.4	−22.5	125.4	10.9
XIX	−10.5	114.6	−24.4	−21.3	157.1	18.1

[a] The interaction energy in solution was evaluated as the sum of the interaction energy in the gas phase computed at the MP2/6-311++G(d,p) level and the $\Delta\Delta G_{assoc}$ estimated for the corresponding solvent (eq 4).

corresponding ion pair is favored by about 31−32 kcal/mol. Conversely, this complexation process is destabilized in aqueous solution by 3−6 kcal/mol. In this case, the large energy penalty arising from the desolvation of the interacting ion ($\Delta\Delta G_{assoc}$) is too large and cannot be compensated by $E_{int,g}$.

The influence of the solvent on the binding of the ion pairs used to mimic PLL·*n*-AS complexes is similar to that described for the reduced models of *n*-ATMA·PALG complexes from a qualitative point of view.[7a] However, a detailed comparison between the two systems reveals important quantitative differences. Thus, the $E_{int,chl}$ values predicted for alkylammonium·alkyl sulfate complexes range from −25.0 to −27.0 kcal/mol, while the values obtained for alkyltrimethylammonium·acetate complexes varied from −2.3 to −3.4 kcal/mol. Therefore, when the trimethylammonium group is replaced by the ammonium one the positive charge is more localized and, as a consequence, the binding in chloroform solution is stabilized by about 22−25 kcal/mol. The difference in the $E_{int,aq}$ values between alkylammonium·alkyl sulfate and alkyltrimethylammonium·acetate complexes amounts to 17−23 kcal/mol, the binding being less favored in the latter than in the former ion pairs. Again, the origin of this difference lies in the charge concentration. The behavior of methylguanidinium·acetate complexes in solution is intermediate between those of alkyltrimethylammonium·acetate and alkylammonium·alkyl sulfate complexes.[2d]

4. Summary

High-level ab initio calculations including electron correlation show that in the gas phase the electrostatic interaction characteristic of PLL·*n*-AS complexes is about 10 kcal/mol stronger than that of *n*-ATMA·PALG complexes but about 5 kcal/mol weaker than that of salt bridges in proteins. The $E_{int,g}$ predicted at the highest computational level employed for the systems under study is approximately −108 kcal/mol.

Calculations in solution show that the bulk solvent plays a crucial role in the binding process. Results indicate that the destabilization induced by solvent is smaller for PLL·*n*-AS than for *n*-ATMA·PALG complexes. Thus, for the former complexes, the attractive energetic contribution in the gas phase partially compensates the destabilizing effect of the solvent. Our calculations predict that in chloroform solution the binding is favored by about 26 kcal/mol for PLL·*n*-AS complexes while only 3 kcal/mol for *n*-ATMA·PALG complexes. In aqueous solution, the binding is unfavored for both types of complexes, but such destabilization is considerably smaller for PLL·*n*-AS than for *n*-ATMA·PALG.

Another fundamental difference was found between the electrostatic interactions of PLL·*n*-AS and *n*-ATMA·PALG complexes. This involves the spatial disposition of the molecular cation with respect to the molecular anion. Thus, an asymmetrical arrangement was reported for *n*-ATMA·PALG complexes, while a symmetric one has been found in the present study for PLL·*n*-AS complexes.

Acknowledgment. Authors are indebted to the Centre de Supercomputació de Catalunya (CESCA) for computational facilities.

Supporting Information Available: Tables providing the distortions energies of the complexes and the optimized geometries and energies of the compounds. This material is available free of charge via the Internet at http://pubs.acs.org.

References and Notes

(1) (a) Riordan, J. F.; McElvany, R. D.; Borders, C. L. *Science* **1977**, *195*, 1977. (b) Raumann, B. E.; Rould, M. A.; Pabo, C. O.; Sauer, R. T. *Nature (London)* **1994**, *367*, 754. (c) Schmirmer, T. E.; Evans, P. R. *Nature (London)* **1990**, *343*, 140. (d) Dym, O.; Mevarech, M.; Sussman, J. L. *Science* **1995**, *267*, 1344 (e) Kumar, S.; Nussinov, R. *Biophys. J.* **2002**, *83*, 1595.

(2) (a) Heidrich, D.; van Eikema Hommes, N. J. R.; von Ragué Schleyer, P. *J. Comput. Chem.* **1993**, *14*, 1149. (b) Zheng, Y.-J.; Ornstein, R. L. *J. Am. Chem. Soc.* **1996**, *118*, 11237. (c) Liljeforrs, T.; Norrby, P. O. *J. Am. Chem. Soc.* **1997**, *119*, 1052. (d) Barril, X.; Alemán, C.; Orozco, M.; Luque, F. J. *Proteins: Struct. Funct. Genet.* **1998**, *32*, 67.

(3) (a) Ponomarenko, E. A.; Waddon, A. J.; Bakeev, K. N.; Tirell, D. A.; MacKnight, W. J. *Macromolecules* **1996**, *29*, 4340. (b) Ponomarenko, E. A.; Waddon, A. J.; Tirrell, D. A.; MacKnight, W. J. *Langmuir* **1996**, *12*, 2169. (c) MacKnight, W. J.; Ponomarenko, E. A.; Tirrell, D. A. *Acc. Chem. Res.* **1998**, *31*, 781.

(4) Ponomarenko, E. A.; Tirrell, D. A.; MacKnight, W. J. *Macromolecules* **1996**, *29*, 8751.

(5) (a) Antonietti, M.; Conrad, J. *Angew. Chem., Int. Ed. Engl.* **1994**, *33*, 18969. (b) Antonietti, M.; Conrad, J.; Thünemann, A. *Macromolecules* **1994**, *27*, 6007. (c) Okuzaki, H.; Osada, Y. *Macromolecules* **1995**, *28*, 380. (d) Kaneko, D.; Olsson, U.; Sakamoto, K. *Langmuir* **2002**, *18*, 4699. (e) Shibata, A.; Ueeno, S.; Ito, Y.; Yamashita, S. *Langmuir* **1998**, *14*, 7519.

(6) (a) Fredickson, G. H. *Macromolecules* **1993**, *26*, 2825. (b) Cao, Y.; Smith, P. *Polymer* **1993**, *34*, 3139.

(7) (a) Zanuy, D.; Alemán, C. *Chem. Phys. Lett.* **2000**, *319*, 318. (b) Zanuy, D.; Alemán, C. *Chem. Phys. Lett.* **2001**, *343*, 390.

(8) (a) Zanuy, D.; Alemán, C.; Muñoz-Guerra, S. *Biopolymers* **2002**, *63*, 151. (b) Zanuy, D.; Alemán, C. *Langmuir*, in press.

(9) Hariharan, P. C.; Pople, J. A. *Theor. Chim. Acta* **1973**, *28*, 213.

(10) Alemán, C. *J. Phys. Chem. A* **2001**, *105*, 860.

(11) Boys, S. F.; Bernardi, F. *Mol. Phys.* **1970**, *19*, 553.

(12) Miertus, S.; Scrocco, E.; Tomasi, J. *Chem. Phys.* **1981**, *55*, 117.

(13) Frisch, M. J.; Trucks, G. W.; Schlegel, H. B.; Scuseria, G. E.; Robb, M. A.; Cheeseman, J. R.; Zakrzewski, V. G.; Montgomery, J. A., Jr.; Stratmann, R. E.; Burant, J. C.; Dapprich, S.; Millam, J. M.; Daniels, A. D.; Kudin, K. N.; Strain, M. C.; Farkas, O.; Tomasi, J.; Barone, V.; Cossi, M.; Cammi, R.; Mennucci, B.; Pomelli, C.; Adamo, C.; Clifford, S.; Ochterski, J.; Petersson, G. A.; Ayala, P. Y.; Cui, Q.; Morokuma, K.; Malick, D. K.; Rabuck, A. D.; Raghavachari, K.; Foresman, J. B.; Cioslowski, J.; Ortiz, J. V.; Stefanov, B. B.; Liu, G.; Liashenko, A.; Piskorz, P.; Komaromi, I.; Gomperts, R.; Martin, R. L.; Fox, D. J.; Keith, T.; Al-Laham, M. A.; Peng, C. Y.; Nanayakkara, A.; Gonzalez, C.; Challacombe, M.; Gill, P. M. W.; Johnson, B. G.; Chen, W.; Wong, M. W.; Andres, J. L.; Head-Gordon, M.; Replogle, E. S.; Pople, J. A. *Gaussian 98*, revision A.7; Gaussian, Inc.: Pittsburgh, PA, 1998.